AN ATTENUATION ADAPTED PULSE COMPRESSION TECHNIQUE TO ENHANCE THE BANDWIDTH AND THE RESOLUTION USING ULTRAFAST ULTRASOUND IMAGING

Yanis Mehdi Benane [1], Denis Bujoreanu [1], Roberto Lavarello [2], Christian Cachard [1], Olivier Basset [1]

[1] Creatis, Univ.Lyon, INSA-Lyon, UCB Lyon 1, UJM-Saint Etienne, CNRS, Inserm, Lyon, France
[2] Laboratorio de Imagenes Medicas, Departamento de Ingenieria, Pontificia Universidad Catolica del Perù

ABSTRACT

Abstract— **Recent studies suggest that Resolution Enhancement Compression (REC) can provide significant improvements in terms of imaging quality over Classical Pulsed (CP) ultrasonic imaging techniques, by employing frequency and amplitude modulated transmitted signals. However the performance of coded excitations methods degrades drastically deeper into the tissue where the attenuation effects become more significant. In this work, a technique that allows overcoming the effects of attenuation on REC imaging is proposed (REC-Opt). It consists in compensating the attenuation effects at each depth in reception. Combined with coherent plane wave compounding (CPWC), REC-Opt was compared to the performance of conventional REC (without attenuation compensation) and CP. With experimental data at 3.25 cm depth in a phantom with an attenuation coefficient slope of 0.5 dB/MHz/cm and using an 8.5 MHz probe, REC-Opt enhanced the bandwidth by 40.6% compared to CP, against an enhancement of only 6% between REC and CP using the same excitation signal designed to provide a 42% increase in bandwidth. The bandwidth enhancements translated into axial resolution improvements of 30% and 3% for REC-Opt vs. CP and REC vs. CP, respectively. This study suggests that REC-Opt is an efficient method to overcome attenuation effects in soft tissues, knowing their attenuation coefficient.**

***Keywords*—Pulse compression, chirp excitation, attenuation compensation, resolution and bandwidth enhancement, experimental results**

1. INTRODUCTION

High-frame-rate ultrasound is a promising imaging modality with several potential clinical applications [1]. For blood flow imaging, this technique has been used to develop ultrafast blood vector velocity imaging [2], which has been applied to the diagnosis of cardiovascular diseases [3-4]. This study proposes to increase the image quality, in terms of resolution and contrast, using coherent plane wave compounding [5] and a coded excitation technique termed resolution enhancement compression (REC) [6]. The REC technique employs amplitude and frequency modulation excitation in order to boost the energy of the backscattered signals in frequency channels where the transducer operates inefficiently. This property of the REC approach makes it a convenient method compared to other pulse compression techniques (eg: conventional chirp [7], Golay codes [8], [9]). Originally, REC was designed for improving the axial resolution of conventional B-mode imaging, which allows to improve lesion detectability [10]. Further, it has been shown that REC, combined with frequency compounding, can also improve image contrast [11]. Although promising results have been reported, the experimental implementation of the technique has been, for a long time, limited to single element transducer systems. The firsts experimental implementations of this technique on an ultrasound array imaging system was obtained, with results showing a successful merge of REC and focused / plane wave ultrasound imaging [12] / [13-15]. REC employs transmitted signals that completely fill the bandwidth of the transducer, therefore, they contain a wide range of frequencies. Since attenuation is a frequency-dependent phenomenon, the spectrum of the ultrasound transmitted signal distorts as the wave propagates deeper inside the tissue. [16]. This effect alters the performance of the REC compression filters [14-15] that fail to compress the backscattered echoes since their bandwidth changes with depth.

In this work, a method that allows adapting the REC compression filters in the presence of attenuation is proposed. Promising results obtained in simulations using Field II [17-18] and experiments using an UlaOp scanner [19] are presented.

2. MATERIAL AND METHODS

1. Coherent plane wave compounding (CPWC)

In ultrafast imaging, a plane wave is generated by firing all transmit elements of the ultrasound probe at once. The generated wave insonifies the whole area of interest. The backscattered echoes are then recorded and processed to compute a complete ultrasound image per transmission at the expense of image quality [5]. The concept of coherent plane wave compounding was introduced in order to solve this drawback [5]. Instead of reconstructing an image from a single plane wave transmission, several plane waves at steering angles $\theta_i \in [\theta_{min}\ \theta_{max}]$ are transmitted into the tissue. Images computed for all θ values are coherently summed to output a single high quality image. To obtain the same image quality as in a standard focused imaging with focal depth Z, the number of plane waves n should be equal to [5]

$$n = \frac{L}{\lambda F^{\#}} \tag{1}$$

where L is the lateral aperture size, λ is the transmitted pulse wavelength, and $F^{\#}=Z/L$ is the F-number. For small steering angles, θ_i can be approximated by

$$\theta_i = \arcsin\left(\frac{i\lambda}{L}\right) \tag{2}$$

with, $i = -(n-1)/2,\ldots,+(n-1)/2$.

2. Resolution enhancement compression (REC)

The REC technique is based on the convolution equivalence principle [6] (see Fig. 1). Assuming that all elements of the probe have approximately the same pulse-echo impulse response, the convolution equivalence principle is given by

$$v_{rec}(t) * h_1(t) = v_{lin}(t) * h_2(t) \tag{3}$$

where $h_1(t)$ is the pulse-echo impulse response of an array element at its focal length (measured experimentally from a reflection of a planar surface immersed in water), $h_2(t)$ describes the designed pulse-echo impulse response with desired properties such as larger spectral support, t represents the time dependence, and $v_{lin}(t)$ is a linear frequency modulated waveform (chirp) that covers the bandwidth of $h_2(t)$. The array elements are excited with a frequency and amplitude modulated waveform $v_{rec}(t)$ called pre-enhanced chirp. By solving (3) in the frequency domain, the pre-enhanced chirp satisfies

$$V_{REC}(f) = V_{LIN}(f) \times \frac{H_2(f)}{H_1(f)} \tag{4}$$

where the capital letters represent the Fourier transform of the corresponding signals. In order to obtain a good approximation of $v_{rec}(t)$, Oelze [6] proposed to replace $H_2(f)/H_1(f)$ by a Wiener filter. $V_{REC}(f)$ becomes

$$V_{REC}(f) = V_{LIN}(f) \times \frac{H_1^*(f) H_2(f)}{|H_1(f)|^2 + |H_1(f)|^{-2}} \tag{5}$$

where $()^*$ denotes complex conjugation. The pre-enhanced chirp $v_{rec}(t)$ was multiplied with a Tukey-cosine window with a 20% taper in order to reduce side-lobe levels, as proposed in [20]. After exciting the source with the pre-enhanced chirp, the received signals are compressed using a modified Wiener filter described by

$$\beta_{REC}(f) = \frac{V_{LIN}^{'*}(f)}{|V_{LIN}^{'}(f)|^2 + \gamma \overline{eSNR}^{-1}(f)} \tag{6}$$

where γ is a smoothing parameter that controls the trade-off between axial resolution and sidelobe levels. $eSNR(f)$ is the echo signal-to-noise ratio per frequency channel. By tapering the $v_{rec}(t)$, the convolution equivalence no longer holds with the original linear FM chirp from (3). Therefore, using a compression filter with the original $v_{lin}(t)$ would yield increased sidelobes. To improve the filter performance, a modified linear FM chirp was used

$$V_{LIN}^{'}(f) = V_{REC}(f) \times \frac{H_1(f)}{H_2(f)} \tag{7}$$

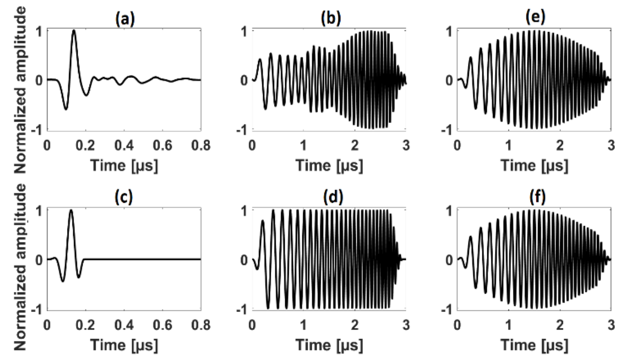

Fig.1. **(a)** & **(c)**, pulses with respectively 91% and 129% −6 dB pulse/echo bandwidth. **(b)**, modified chirp used to excite the 91% bandwidth source. **(d)**, linear chirp used to excite the 129% bandwidth source. **(e)** & **(f)**, Convolution of the pulses with their respective chirps sequences.

3. Attenuation compensation

In our previous works [14-15] we concluded that the Wiener filter in (6) used for REC compression becomes less effective deeper into the media where echoes travel longer distances thus are more affected by attenuation. The idea here is to model attenuation by its impulse response $h_{att}(t,d)$, where t represents the time and d stands for the forward/backward propagation distance of the signal between the transducer and the scattering point. By introducing $h_{att}(t,d)$ in (3), the equivalence between the transmission of the pre-enhanced chirp by the real transducer (of bandwidth $h_1(t,x)$) and the transmission of the linear chirp by the desired transducer (of bandwidth $h_2(t,x)$) holds for each point at the distance d in presence of attenuation, i.e.,

$$v_{rec}(t) * h_1(t) * h_{att}(t,d) = v_{lin}(t) * h_2(t) \tag{8}$$

In the Fourier domain (8) becomes

$$V_{REC}(f) \times H_1(f) \times H_{att}(f,d) = V_{LIN}(f) \times H_2(f), \tag{9}$$

$H_{att}(f,d)$, the Fourier transform of $h_{att}(t,d)$, is given by [16]

$$H_{att}(f,d) = exp(-\alpha d|f|)\, exp(-j2\pi f \tau d)\, exp\left(j\frac{2f\alpha d}{\pi} ln(2\pi f)\right), \tag{10}$$

$$\tau = \tau_b + \frac{\alpha}{\pi^2}\tau_m$$

where α is the attenuation coefficient slope, τ_b is the bulk delay, and τ_m is the minimum-phase delay factor. In [16] the authors proposed to use $\tau_m = 20$ and $\tau_b = 6.67$µs/cm in order to fit the dispersion in the soft tissues. In this work, α was assumed to be constant and known. In (9) one can observe that $H_1(f) \times H_{att}(f,d)$ can be replaced with a single term $H_{1att}(f,d)$. Therefore, in this study in order to account for attenuation effects (7) and (6) have been modified as

$$V'_{LIN}(f,d) = V_{REC}(f) \times \frac{H_{1att}(f,d)}{H_2(f)} \tag{11}$$

$$\beta_{REC}(f,d) = \frac{V'^{*}_{LIN}(f,d)}{\left|V'_{LIN}(f,d)\right|^2 + \gamma \overline{eSNR}^{-1}(f)} \tag{12}$$

Note that in (12) the new compression filter depends on the travel distance in the medium, thus a different filter has to be calculated for each depth in the received signals. For this study, a pointwise compression of the received signals with the corresponding $\beta_{REC}(f,d)$ has been performed.

3. SIMULATION RESULTS

In order to validate the theory described in Section 2, simulations were performed using CPWC. Two different excitations were used: CP with a half sinusoid at the center frequency of the impulse response of the probe (8.5 MHz), and a pre-enhanced chirp (Fig.1 (b)). In the second case, the received signals were compressed using $\beta_{REC}(f)$ for REC and using $\beta_{REC}(f,d)$ for REC-Opt. The simulation was conducted using Field II [14], [15]. An angular aperture of 18° was divided in 27 directions equally spaced by 0.67° (in accordance with Section 2.1). On the ultrasound probe, only the 64 central elements were used for both transmit and receive. The medium contained six scatterers arranged on two horizontal lines at depths of 4 cm and 5 cm. The simulated medium had an attenuation coefficient slope of 0.5dB/MHz/cm, which is comparable to the value in the human liver. Additive white Gaussian noise (AWGN, SNR $\approx$ 20 dB) was added to the RF data prior to beamforming (for CP) and prior to compression (for REC and REC-Opt) in order to evaluate the approach in presence of observation noise. The obtained B-mode images for the different techniques are shown in Fig. 2.

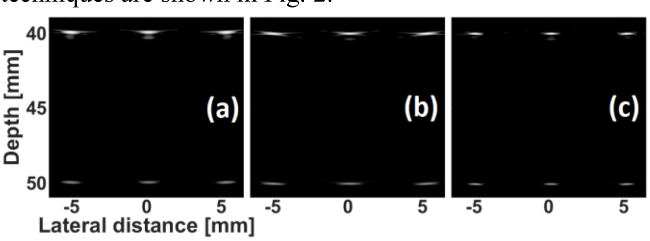

Fig.2. Log-compressed B-mode images of a simulated wire phantom obtained with **CP** (a), **REC** (b) and **REC-Opt** (c) using 27 plane waves. All images have a dynamic range of 55 dB.

It can be visually observed that REC-Opt allowed obtaining a better spatial resolution than REC and CP. The choice of γ (γ = 50) for REC and REC-Opt was made with the aim of obtaining the best axial resolution possible while preserving a noise level below the one of CP. A difference of about 15 dB can be observed between noise level of CP regarding to REC and REC-Opt (Fig.3 (a)). As shown in Fig. 3(b), the improvement concerning the axial resolution was quantified through the calculation of the modulation transfer function (MTF) derived from the envelope data. In particular, the wave numbers k_{-20dB} at which the MTFs dropped below -20 dB were 35, 37.1 and 45.2 mm^{-1} for CP, REC and REC-Opt, respectively. The power spectra of the reflection from the wire at a depth of 4 cm are shown in Fig. 3(c). In accordance with the improvements in the MTF, the -6 dB bandwidths were 3.88, 4.14 and 5.45 MHz, respectively. These results correspond to enhancements in axial resolution and bandwidth between REC-Opt and CP of 30 % and 40.5%, respectively.

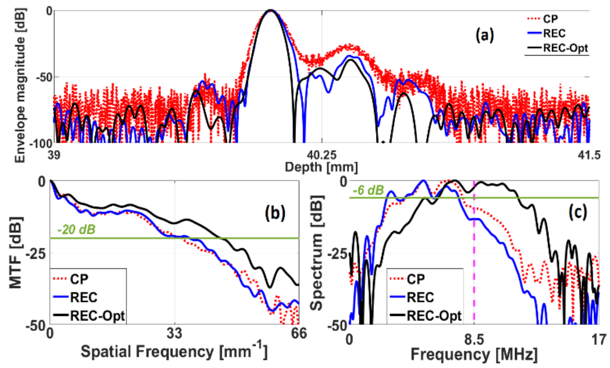

Fig.3. Comparison of performance between REC-Opt (solid black line), REC (solid blue line) and CP (dashed red line). (a) Envelope of the radiofrequency data of the scatterer placed at 4 cm depth in the center of the image. (b) MTF derived from (a). (c) Normalized spectrum derived from the radiofrequency data of the same scatterer.

4. EXPERIMENTAL RESULTS

For the data acquisition, the open ultrasound platform UlaOp (Microelectronics System Design Lab, Florence, Italy) equipped with a LA523E linear array probe (Esaote, Genova, Italy) was used. The UlaOp can transmit arbitrary waveforms and define customized transmissions and reception strategies [16]. The probe has 192 elements (pitch = 0.245 mm) and is centered at 8.5 MHz. The experimental acquisitions were conducted with the same parameters as in simulation. The phantom studied (model 410SCG HE 0.5 Gammex Sun nuclear, Neu-Isenburg, Germany) has an attenuation coefficient slope of 0.5 dB/MHz/cm.

1. Wire phantom

The first experiment consists on imaging a phantom that contains two wires of 100 µm thickness, placed at 2.25 cm and 3.25 cm depth. The obtained B-mode images using the three different techniques are shown in Fig. 4.

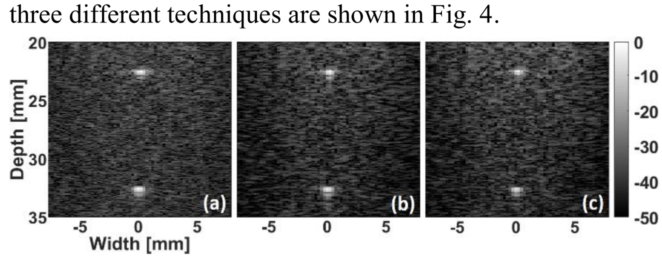

Fig.4. Log-compressed B-mode images of wire phantom obtained with **CP** (a), **REC** (b) and **REC-Opt** (c) using 27 plane waves.

One can observe that REC-Opt provided the best image quality among the three techniques. This is particularly noticeable by the lower thickness of the points corresponding to the two wire targets. This effect is confirmed by studying the axial resolution and the spectrum derived from the radiofrequency data of the wire placed at 32.5mm (Fig.5). The MTF values were 14.4, 14.85 and 18.71 mm^{-1} (which corresponds to a resolution of respectively 218.2, 211.6 and 167.9 μm) for CP, REC and REC-Opt, respectively. Therefore, the axial resolution was improved by 30% between REC-Opt and CP and by 26% between REC-Opt and REC. In accordance with the improvements in the MTF, the -6 dB bandwidths were estimated to be 2.54, 2.61 and 3.57 MHz for CP, REC and REC-Opt, respectively. Because of the attenuation in the medium (0.5dB/MHz/cm) at this depth (3.25 cm), REC is no longer effective and gives almost the same performance in axial resolution and bandwidth as CP.

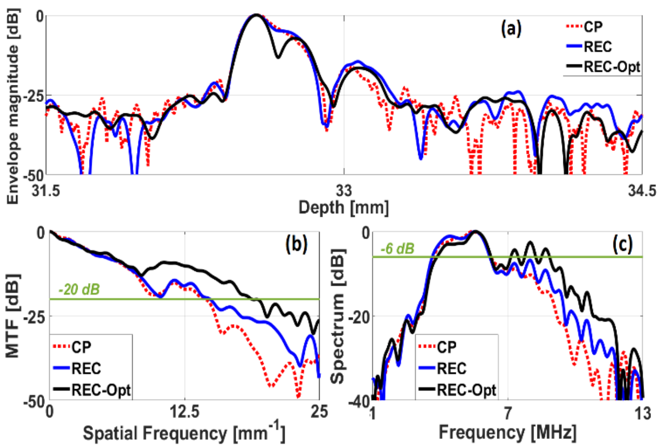

Fig. 5. Comparison of performance between REC-Opt (solid black line), REC (solid blue line) and CP (dashed red line). (a) Envelope of the radiofrequency data of the scatterer placed at 3.25 cm. (b) MTF derived from the envelope. (c) Normalized spectrum derived from the radiofrequency data.

2. Cyst phantom

The proposed method was also evaluated experimentally by imaging hypoechoic cyst placed at 4cm depth from the same phantom. Fig. 6 shows the obtained B-mode images.

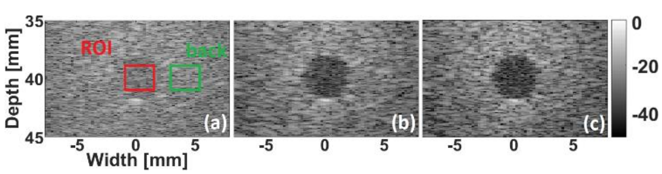

Fig.6. Log-compressed B-mode images of hypoechoic cyst at 4cm depth obtained with **CP** (a), **REC** (b) and **REC-Opt** (c) using 27 plane waves.

The results clearly show an improvement in terms of image quality between CP and REC/REC-Opt. A slight improvement is also noted between REC and REC-Opt, especially concerning the contrast and the speckle size. To quantify the image quality, the speckle signal-to-noise ratio (SNR) and the contrast-to-noise ratio (CNR) were computed. SNR was defined as the ratio between the mean μ_{ROI} and the standard deviation σ_{ROI} of the image amplitude in a region of interest (ROI). The CNR was defined as $|\mu_{ROI} - \mu_{back}| / \sqrt{\sigma_{ROI}^2 + \sigma_{back}^2}$. The obtained values of CNR and SNR calculated using the square areas (Fig.4) are depicted in Table I. By compensating the attenuation, the new approach improves the CNR and SNR by respectively 1.17 and 2.1 dB in comparison with REC.

Table I: Metrics comparison

	CP	REC	**REC-Opt**
CNR *(dB)*	-4,31	4,32	**5,49**
SNR *(dB)*	14,8	16,1	**18,2**

5. DISCUSSION AND CONCLUSION

The results obtained from wire phantoms showed clearly the limits of REC in presence of attenuation. Only 6.7% / 2.8% improvements respectively in axial resolution / bandwidth were observed experimentally between REC and CP. The same behavior was observed in simulation with only 6% / 3.1% enhancements. These problems were solved when the attenuation of the medium was taken into account. Indeed, the results obtained with both simulations and experiments led in bandwidth improvements (i.e., 40.5% and 40.6%, respectively) of REC-Opt in comparison to CP, consistent with the intended bandwidth boost of 42%. The improvement in the spatial resolution of the wire profiles (i.e., 29 and 30% for simulation and experiment as quantified with the k_{-20}dB value derived from the MTF curves) was also consistent with the intended bandwidth improvement. By adapting the compression filter, the proposed approach (REC-Opt) was also capable to improve the CNR by 27% and SNR by 13% compared to REC. In the presented work, the pre-enhanced chirp excitation was designed to achieve only a modest increase in bandwidth. This was due to the aspect of the transducer impulse response spectrum, which decreases sharply at the high frequencies (at around 13 MHz). The experimental results suggest that the REC technique adapted to the medium attenuation (REC-Opt) provides a better image quality than the classical REC technique for ultrasonic imaging.

AKNOWLEDGMENT

This work was performed within the framework of the ANR-11 TecSan-008–01 BBMUT and was supported by LABEX CELYA (ANR-10-LABX-0060) and LABEX PRIMES (ANR-10-LABX-0063), within the program "Investissements d'Avenir" (ANR-11-IDEX-0007) operated by the French National Research Agency (ANR).

This work was also supported by the Fondo Nacional de Desarrollo Científico y Tecnológico-PERU under grant 012-2014-FONDECYT-C1 from the Peruvian Government.

6. REFERENCES

[1] M. Tanter and M. Fink, "Ultrafast imaging in biomedical ultrasound," *IEEE Transactions on Ultrasonics, Ferroelectrics and Frequency Control, vol. 61, no. 1, pp. 102–119, 2014.*

[2] J. Udesen, F. Gran, K. L. Hansen, J. A. Jensen, C. Thomsen, and M. B. Nielsen, "High frame-rate blood vector velocity imaging using plane waves: simulations and preliminary experiments," *IEEE Transactions on Ultrasonics, Ferroelectrics and Frequency Control, vol. 55, no. 8, pp. 1729–1743, 2008.*

[3] B.-F. Osmanski, M. Pernot, G. Montaldo, A. Bel, E. Messas, and M. Tanter, "Ultrafast Doppler imaging of blood flow dynamics in the myocardium," *IEEE Trans. Med. Imaging, vol. 31, no. 8, pp. 1661–1668, 2012.*

[4] M. Couade, M. Pernot, M. Tanter, E. Messas, A. Bel, M. Ba, A.-A. Hagege, and M. Fink, "Ultrafast imaging of the heart using circular wave synthetic imaging with phased arrays," *in IEEE International Ultrasonics Symposium (IUS), IEEE International, 2009, pp. 515–518.*

[5] G. Montaldo, M. Tanter, J. Bercoff, N. Benech and M. Fink "Coherent Plane-Wave Compounding for Very High Frame Rate Ultrasonography and Transient Elastography," *IEEE Transactions on Ultrasonics, Ferroelectrics and Frequency Control, vol. 56, no. 3, pp. 489-506, 2009.*

[6] M. Oelze, "Bandwidth and resolution enhancement through pulse compression," *IEEE Transactions on Ultrasonics, Ferroelectrics and Frequency Control, vol. 54, no. 4, pp. 768–781, 2007.*

[7] M. H. Pedersen, T. X. Misaridis, and J. A. Jensen "Clinical evaluation of chirp-coded excitation in medical ultrasound," *Ultrasound in medicine & biology, vol. 29, no.6, pp. 895-905, 2003.*

[8] I. Trots, and A. Nowicki "Influence of the transducer bandwidth on compressed ultrasonic echoes," *Archives of Acoustics, vol. 32, no.4, pp. 903-915, 2007.*

[9] A. Nowicki, I. Trots, P. A. Lewin, W. Secomski, and R. Tymkiewicz "Influence of the ultrasound transducer bandwidth on selection of the complementary Golay bit code length, Ultrasonics," *vol. 47, no.1, pp. 64-73, 2007.*

[10] P. Linden, J. R. Sanchez, and M. L. Oelze, "Small lesion detection with resolution enhancement compression," Ultrasonic Imaging, vol. 32, no. 1, pp. 16–32, 2010.

[11] J. R. Sanchez and M. Oelze, "An ultrasonic imaging speckle-suppression and contrast-enhancement technique by means of frequency compounding and coded excitation," *IEEE Transactions on Ultrasonics, Ferroelectrics and Frequency Control, vol. 56, no. 7, pp. 1327–1339, 2009.*

[12] F. Lin, J. Sanchez, C. Cachard, O. Basset, and R. Lavarello, "First experimental implementation of a bandwidth enhancement pulse compression technique on an ultrasound array imaging system," *Biomedical Imaging ISBI, pp. 1188–1191, 2014.*

[13] S. Salles, F. Varray, Y. M. Benane and O. Basset, "Optimization of resolution enhancement compression technique with plane wave imaging," *in IEEE International Ultrasonics Symposium (IUS), 2017.*

[14] Y. M. Benane, R. Lavarello, D. Bujoreanu, C. Cachard, F. Varray, J-M Escoffre, Anthony Novell and O. Basset, "Ultrafast Ultrasound Imaging using a Resolution and Bandwidth enhancement Technique," *in IEEE International Ultrasonics Symposium (IUS), 2017.*

[15] Y. M. Benane, R. Lavarello, D. Bujoreanu, C. Cachard, A. S. Savoia, E. Franceschini and O. Basset, "Ultrasound Bandwidth Enhancement Through Pulse Compression Using a CMUT Probe," *in IEEE International Ultrasonics Symposium (IUS), 2017.*

[16] K. V. Gurumurthy, and R. Martin Arthur "A dispersive model for the propagation of ultrasound in soft tissue," *Ultrasonic Imaging, vol. 4, no. 4, pp. 355–377, 1982.*

[17] J.A. Jensen: "Field: A Program for Simulating Ultrasound Systems," *Medical & Biological Engineering & Computing, vol. 34, Supplement 1, Part 1, pp. 351-353, 1996.*

[18] J.A. Jensen and N. B. Svendsen: "Calculation of pressure fields from arbitrarily shaped, apodized, and excited ultrasound transducers," *IEEE Transactions on Ultrasonics, Ferroelectrics and Frequency Control, vol. 39, no.2, pp. 262-267, 1992.*

[19] P. Tortoli, L. Bassi, E. Boni, A. Dallai, F. Guidi, and S. Ricci, "ULA-OP: an advanced open platform for ultrasound research," *IEEE Transactions on Ultrasonics, Ferroelectrics and Frequency Control, vol. 56, no. 10, pp. 2207–2216, 2009.*

[20] R. Y. Chiao and X. Hao, "Coded excitation for diagnostic ultrasound: A system developer's perspective," *IEEE Transactions on Ultrasonics, Ferroelectrics and Frequency Control, vol. 52, pp. 160–170, 2005.*